

Plasma-Induced Formation of Ag Nanodots for Ultra-High-Enhancement Surface-Enhanced Raman Scattering Substrates

Zhiyong Li,^{*,†} William M. Tong,^{†,‡} William F. Stickle,[§] David L. Neiman,[§] and R. Stanley Williams[†]

Quantum Science Research, Hewlett-Packard Laboratories, 1501 Page Mill Road, Palo Alto, California 94304, Advanced Materials Process Lab and Advanced Diagnostic Lab, Hewlett-Packard Company, Corvallis, Oregon 97330

Luke L. Hunter and A. Alec Talin

Sandia National Laboratories, Livermore, California 94550

D. Li and S. R. J. Brueck

Center for High Technology Materials, University of New Mexico, Albuquerque, New Mexico 87106

Received December 20, 2006. In Final Form: February 13, 2007

We report here plasma-induced formation of Ag nanostructures for surface-enhanced Raman scattering (SERS) applications. An array of uniform Ag patterned structures of 150 nm diameter was first fabricated on a silicon substrate with imprint lithography; then the substrate was further treated with an oxygen plasma to fracture the patterned structures into clusters of smaller, interconnected, closely packed Ag nanoparticles (20–60 nm) and redeposited Ag nanodots (~10 nm) between the clusters. The substrate thus formed had a uniform ultrahigh SERS enhancement factor (10^{10}) over the entire substrate for 4-mercaptophenol molecules. By comparison, Au patterned structures fabricated with the same method did not undergo such a morphological change after the plasma treatment and showed no enhancement of Raman scattering.

For 30 years, surface-enhanced Raman scattering (SERS) has attracted considerable interest because of its great potential for trace chemical analysis. One critical issue limiting the general application of SERS is the economical fabrication of a uniform SERS substrate. Numerous efforts have been devoted to the search for a uniform, repeatable, manufacturable SERS substrate with enormous enhancement factors that were observed in random “hot spots.”¹ The importance of geometry and the separation between metallic nanostructures was recognized soon after the initial emphasis of generating rough metal surfaces.^{2–4} Both theoretical and experimental studies indicated that a controlled separation of less than 5 nm between aggregated nanoparticles is one of the important characteristics of strongly enhancing SERS substrates,⁵ but this is beyond the resolution of any scalable top-down fabrication approach. Assembling metal nanostructures synthesized by a bottom-up approach, such as by Langmuir–Blodgett films or by casting metal colloids onto surfaces, can achieve regular arrays of metallic nanoparticles or nanowires with small separation,^{6,7} but this approach usually requires a monolayer coating of surfactants for dispersion during synthesis,

which can interfere with the Raman signal of the analyte, and does not have sufficient control of the size and separation. Other techniques, such as nanosphere lithography, based on the use of close-packed nanospheres as the lift-off layer for evaporated Ag, also fail to provide the necessary nanometer-scale gaps between metallic nanostructures.⁸ With its rapid cycle time, extendability to roll-to-roll printing,⁹ and demonstrated sub 10 nm resolution,¹⁰ nanoimprinting lithography (NIL) would appear to be the natural choice for large-scale manufacturing of SERS substrates. However, as we show in this paper, at the ~150 nm feature size, NIL alone is not sufficient to provide the very high enhancement desirable for SERS detection. Rather, we report on a hybrid method that utilizes first NIL to achieve coarse (~400 nm) separation between 150 nm Ag metallic patterned structures over a large substrate area and then a simple oxygen-plasma treatment to produce Ag nanodots, which yielded surprisingly uniform and reliable high enhancement factors for Raman scattering.

Patterned Au and Ag structures were fabricated on thermally oxidized (100 nm SiO₂) silicon substrates with NIL, which is a top-down technique based on stamping a hard mold into a polymer that is either thermally or UV cured. NIL is ideally suited to define nanoscale patterns over large fields and with high

* To whom correspondence should be addressed. E-mail: zhiyong.li@hp.com.

[†] Hewlett-Packard Laboratories.

[‡] Advanced Materials Process Lab, Hewlett-Packard Co.

[§] Advanced Diagnostic Lab, Hewlett-Packard Co.

(1) Nie, S.; Emory, S. R. *Science* **1997**, *275*, 1102.

(2) Jeanmaire, D. L.; Van Duyne, R. P. *J. Electroanal. Chem.* **1977**, *84*, 1–20.

(3) McCall, S. L.; Platzman, P. M.; Wolff, P. A. *Phys. Lett.* **1980**, *77*, 381–383.

(4) Moskovits, M. *J. Chem. Phys.* **1978**, *69*, 4159.

(5) Jiang, J.; Bosnick, K.; Maillard, M.; Brus, L. *J. Phys. Chem. B* **2003**, *107*, 9964.

(6) Wang, H.; Levin, C. S.; Halas, N. *J. Am. Chem. Soc.* **2005**, *127*, 14992.

(7) Tao, A.; Kim, F.; Hess, C.; Goldberger, J.; He, R.; Sun, Y.; Xia, Y.; Yang, P. *Nano Lett.* **2003**, *3*, 1229–1233.

(8) Haes, A. J.; Haynes, C. L.; McFarland, A. D.; Schatz, G. C.; Van Duyne, R. P.; Zou, S. *MRS Bull.* **2005**, *30*, 368.

(9) Schiff, H.; Heyderman, L. J. In *Alternative Lithography: Unleashing the Potentials of Nanotechnology*; Sotomayor, C. M., Ed.; Kluwer Academic: Dordrecht, The Netherlands, 2003; p 50.

(10) Chou, S. Y. In *Alternative Lithography: Unleashing the Potentials of Nanotechnology*; Sotomayor, C. M., Ed.; Kluwer Academic: Dordrecht, The Netherlands, 2003; p 15.

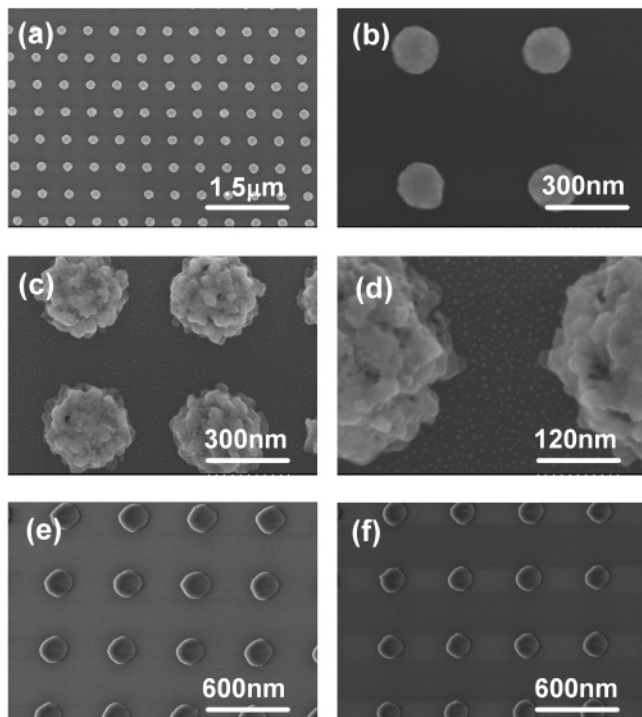


Figure 1. SEM images of (a) as-patterned Ag structures by imprinting lithography, (b) a magnified view of the patterned Ag structures as shown in (a), (c) an oxygen-plasma-treated sample, and (d) a magnified view of the oxygen-plasma-treated sample, showing the presence of small nanodots. SEM images of a gold sample before (e) and after (f) the same oxygen-plasma treatment are shown for comparison.

resolution and throughput.^{11,12} In this work we used a SiO₂ on Si mold fabricated by a combination of laser interference lithography and reactive ion etching.¹³ The utilization of interference lithography for mold fabrication has the advantage of patterning large-area samples at low cost. This mold was used on a Nanonex2000 commercial NIL tool to pattern 300 nm thick PMMA at 130 °C and a pressure of 200 psi. The patterning of PMMA only required ~5 min. After imprinting, the substrates were etched for 20 s in an oxygen plasma at 50 W to remove residual PMMA; this was followed by evaporation of either 6 nm Cr/60 nm Au or 6 nm Ti/60 nm Ag. The film thickness was monitored with a quartz crystal monitor and was independently verified by cross-sectional scanning electron microscopy. The metal pattern was created by lift-off with ultrasound in an acetone bath. Parts a, b, and e of Figure 1 show SEM images of the as-patterned Ag and Au structures, indicating the well-controlled size of 150 nm in diameter and separation of 400 nm. Oxygen-plasma treatment of the Ag and Au patterned structures was carried out in a March parallel plate etcher at an oxygen pressure of 0.5 Torr, 50 W power, for a duration of 1 min. Figure 1c is the same patterned Ag structure after the oxygen-plasma treatment, showing significant roughening. Careful examination of the high-resolution SEM image (Figure 1d) revealed that the patterned structures had both increased in size and fractured into interconnected nanoparticles 40 ± 20 nm in diameter, which is typical of the grain size observed for 60 nm Ag films.¹⁴ Furthermore, on the substrate, we observed the presence of isolated

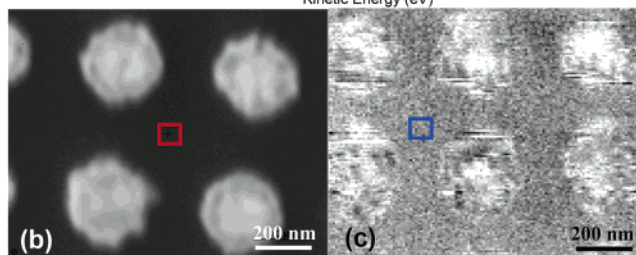
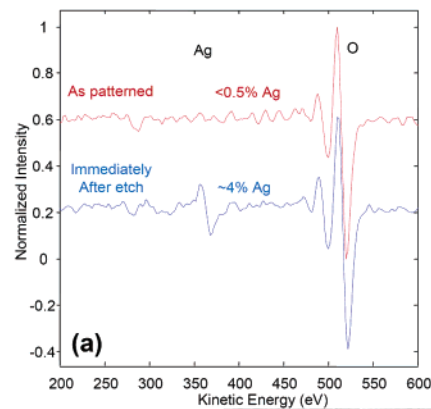


Figure 2. (a) Representative Auger spectra of the SiO₂ substrate area from the red and blue square regions in (b) and (c), showing that Ag was redeposited onto the substrate even though the nanodots were not observed. The oxygen peak came from the silicon oxide layer of the substrate. (b, c) Auger intensity maps at a 360 eV kinetic energy of the samples before and immediately after oxygen-plasma treatment, respectively.

Ag nanodots of average size of 10 nm and of average height of 8 nm (measured by atomic force microscopy). Similar fracturing and redeposition were observed for samples that were aggressively etched by Ar ions, suggesting that Ar-plasma etching may also be used to produce such structures, but probably with less control. However, the formation of the nanodots and the fracturing of the patterned structures were not observed in the Au case, as shown in parts e and f of Figure 1 for before and after the oxygen-plasma treatment, respectively. The fracturing of the Ag patterned structures into distinguishable nanoparticles was likely due to the grain boundaries widened by the oxygen plasma. For Au, we believe that the lack of large grain boundaries and the stronger metallic bonding energy in Au are why its patterned structures did not undergo the same fracturing.

On the other hand, the mechanism of formation for the Ag nanodots was initially a mystery because of the difficulty in resolving them even with a high-resolution scanning electron microscope and also because they did not appear immediately after the oxygen-plasma treatment. We compared Auger spectra on the SiO₂ substrate area of the Ag samples immediately after oxygen-plasma treatment and discovered the presence of Ag, as shown in Figure 2. Despite the lack of any nanodots observable by SEM, a silver film was redeposited from the patterned Ag structure by the oxygen plasma. Once the plasma was turned off, the film, which was likely to be composed of Ag₂O during its initial formation, decomposed into Ag on the substrate and left a thin film of Ag behind. Like all metals, Ag has a very high surface energy. However, unlike other metals, Ag has a high surface mobility even at room temperature. It took less than a day for the silver film to self-coalesce into small islands to reduce its surface energy. The average separation of the nanodots induced by this plasma treatment was measured to be approximately 20 nm from the high-resolution SEM images.

(11) Chou, S. Y.; Krauss, P. R.; Renstrom, P. J. *Science* **1996**, *272*, 85.

(12) Chen, Y.; Jung, G. Y.; Ohlberg, D. D. A.; Li, X.; Stewart, D. R.; Jeppesen, J. O.; Nielsen, K. A.; Stoddart, J. F.; Williams, R. S. *Nanotechnology* **2003**, *14*, 462.

(13) Brueck, S. R. J. *Proc. IEEE* **2005**, *93*, 1704.

(14) Maqbool, M.; Khan, T. *Surf. Rev. Lett.* **2005**, *12*, 759–766.

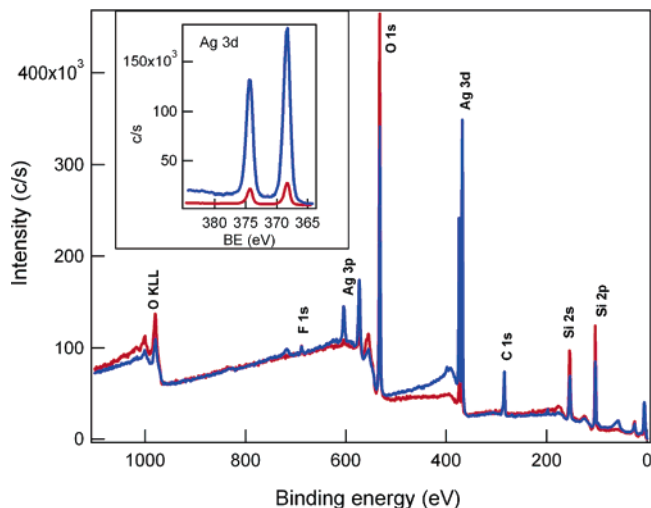


Figure 3. XPS survey spectra of the as-patterned (red) and the oxygen-plasma-treated (blue) Ag patterned structures. The inset shows the high-resolution spectra of the Ag 3d region from the two samples.

The as-patterned and the oxygen-plasma-treated samples were analyzed by X-ray photoelectron spectroscopy. As shown in Figure 3, other than a small amount of silver oxide, the chemical composition was not changed by the oxygen-plasma treatment. Interestingly, the oxygen-plasma-treated sample showed much greater intensity for the Ag peaks than the untreated Ag patterned structure (see the Ag 3d high-resolution spectra in the inset of Figure 3), while much less intense oxygen 1s and silicon 2s and 2p peaks were observed. This can be attributed to the silicon oxide substrate being covered by the redeposited Ag after oxygen-plasma treatment. A trace amount of fluorine 1s peak in the spectrum of the oxygen-plasma-treated Ag sample was likely due to contamination of the oxygen-plasma process. Its intensity diminished after the sample was simply rinsed with ethanol.

For SERS evaluation, the samples were soaked in 1 μ M 4-mercaptophenol in ethanol solution for 10 min, rinsed with fresh ethanol, and blown dry with nitrogen. The Raman spectra of the samples were collected on a Horiba-Yvon T64000 micro Raman system, with three laser excitation sources at 532, 633, and 785 nm. The intensity of the laser incident on the sample surface was measured to be about 2.1, 1.2, and 2.2 mW for 532, 633, and 785 nm lasers, respectively, over a focused area of roughly 1 μ m² through a 100 \times objective. Each Raman spectrum was averaged over 10 acquisitions with a 2 s collection time. The Raman shift at 520 cm^{-1} , assigned to the Si substrate phonon, served as an internal standard for the calibration of both the Raman shifts and the intensity of the molecular peaks. The plasma-treated Ag patterned structures consistently yielded highly enhanced spectra of the mercaptophenol molecules on the surface for all three excitation wavelengths, as shown in Figure 4. In comparison, the as-patterned Ag samples barely generated any detectable signal associated with mercaptophenol molecules within the instrument sensitivity at the 633 and 785 nm excitations, whereas the silicon peaks were of comparable intensity for both the as-patterned Ag samples and the plasma-treated samples. Excitation at 532 nm yielded noticeable molecular vibration peaks for the as-patterned Ag sample but still with much lower intensity as compared to those for the oxygen-plasma-treated sample.

To understand the relative contributions to the enhancement by the fractured nanoparticles on the patterned structures and the nanodots on the substrates, we carried out a controlled experiment by performing the oxygen treatment on the film before the lift-off, thereby producing only the fractured nanoparticles without

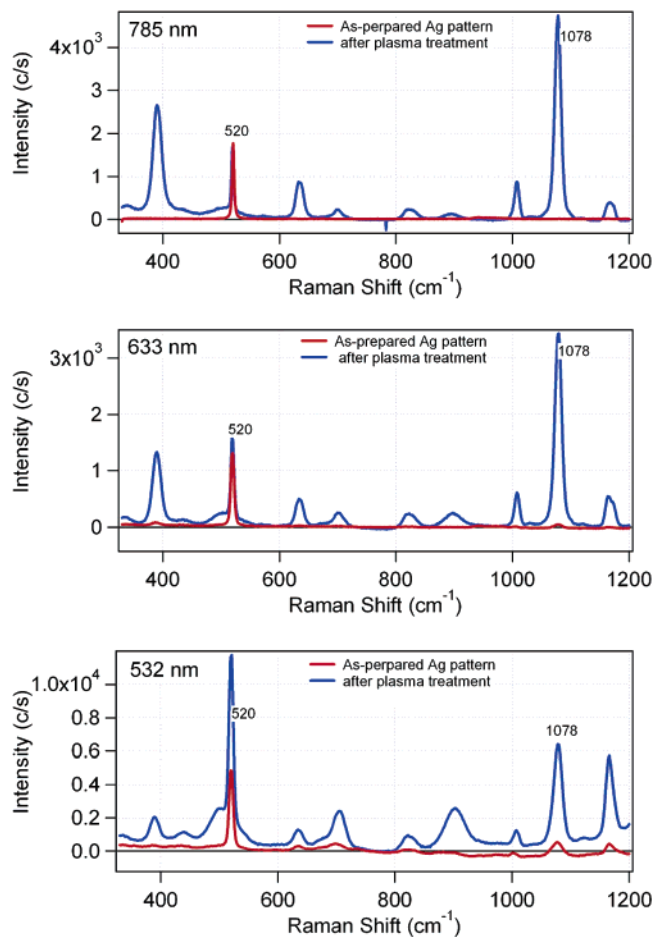


Figure 4. Raman spectra of 4-mercaptophenol adsorbed onto the as-patterned (red curves) and the oxygen-plasma-treated (blue curves) Ag structures at three excitation wavelengths, 785 nm (top), 633 nm (middle), and 532 nm (bottom).

the nanodots on the substrate. This substrate demonstrated very weak Raman activity, thus suggesting that the enhancement mainly originates from the nanodot substrate.

To calculate the enhancement factor from the nanodot substrate, we also collected the Raman spectra of neat 4-mercaptophenol in a quartz liquid cell using the same micro Raman system at three excitation wavelengths. The enhancement factor was calculated by the equation $EF = (I_{\text{SERS}}/I_{\text{neat}})(M_{\text{neat}}/M_{\text{SERS}})$, where I_{SERS} and I_{neat} are Raman peak intensities normalized by the laser power density for both the SERS substrate and neat sample, respectively, and M_{SERS} and M_{neat} are the total numbers of molecules exposed under the laser spot.

Assuming a monolayer coverage of mercaptophenol molecules on the Ag surface of 10¹³/cm², we obtained an enhancement factor of 6 \times 10⁹, 1 \times 10¹⁰, and 7 \times 10¹⁰ for the peak at 1078 cm^{-1} at 532, 633, and 785 nm excitation, respectively. An area mapping Raman scan of the plasma-treated Ag nanodot substrate showed a standard deviation of 37% of the enhancement factor in a 100 μ m \times 100 μ m region, indicating a good uniformity of the SERS effect in such a substrate. The stability of the plasma-treated Ag substrate was also evaluated by storing the plasma-treated substrate in an ambient lab environment over a month and then repeating the Raman study. No appreciable change was observed on the SERS spectra for the mercaptophenol molecules on the aged sample.

The enhancement factor is partly contributed by an intense electromagnetic field generated by the surface plasmons; large signal enhancement is normally achieved at the excitation

coincident with the surface-plasmon resonance frequency, which is in turn determined by the size, geometry, and separation of the Ag nanostructures.^{4,15–17} For isolated Ag nanoparticles, the electromagnetic field mechanism can only account for an average enhancement factor of 10^6 , and the highest Raman enhancement factor for single Ag spheres was found for particles with a 20–25 nm radius.^{18,19} Only when there is a 1 nm separation between aggregated Ag nanoparticles,⁵ the enhancement factor can be as high as 10^{10} to 10^{12} . For our nanodots induced by plasma treatment, which have an average radius of 5 nm and are separated by large gaps (>20 nm), the local surface plasmon effect alone seems not be able to account for the large observed enhancement (10^{10}). Recently, Zou and Schatz²⁰ have reported that the periodic array of nanoparticles, which combine particle plasmon excitation with long-range photonic interactions, can generate a large enhancement factor of 10^{13} . The contribution other than the

nanodots themselves in the plasma-treated periodic Ag pattern substrate is currently under investigation.

In summary, we have demonstrated a new method of fabricating a SERS substrate with reliable and uniform ultrahigh enhancement. This method was based on the simple oxygen-plasma-induced formation of Ag nanoparticles and nanodots from Ag patterned structures fabricated economically with nanoimprint lithography. While we observed both the fracturing of the Ag structures into nanoparticles and the redeposition of the Ag nanodots on the substrate, the nanodots are believed to be mainly responsible for the intense Raman enhancement. The mechanism of formation for the nanodots is believed to be the coalescence of a thin Ag film that had been redeposited under oxygen-plasma treatment. The size and separation of the nanodots were dictated by the diffusion-limited aggregation of Ag atoms.

(15) Wenseleers, W.; Stellacci, F.; Meyer-Friedrichsen, T.; Mangel, T.; Bauer, C. A.; Pond, S. J. K.; Marder, S. R.; Perry, J. W. *J. Phys. Chem. B* **2002**, *106*, 6853–6863.

(16) Wang, Z.; Pan, S.; Krauss, T. D.; Du, H.; Rothberg, L. J. *Proc. Natl. Acad. Sci. U.S.A.* **2003**, *100*, 8638–8643.

(17) Yang, W. H.; Schatz, G. C.; Van Duyne, R. P. *J. Chem. Phys.* **1995**, *103*, 869.

(18) Messinger, B. J.; von Raben, K. U.; Chang, R. K.; Barber, P. W. *Phys. Rev. B* **1981**, *24*, 649.

(19) Wokaun, A.; Gordon, J. P.; Liao, P. F. *Phys. Rev. Lett.* **1982**, *48*, 957.

(20) Zou, S.; Schatz, G. C. *Chem. Phys. Lett.* **2005**, *403*, 62.

Acknowledgment. Sandia is a multiprogram laboratory operated by Sandia Corp., a Lockheed-Martin company, for the U.S. Department of Energy National Nuclear Security Administration under Contract DE-AC04-94AL85000. The facilities of the NSF-sponsored NNIN at the University of New Mexico were used for the imprint master fabrication.

LA063688N